A Search for Baroclinic Structures

Alexander E. Hasha

August 26th, 2005

1 Introduction

The calculation reported in this paper is a standard one for those who study pattern formation in nonlinear systems. Pattern formation is prevalent when instability breaks symmetries present in a basic state. In the canonical example, stationary fluid heated from below gives way to patterns through Rayleigh-Bénard instability. For a wide class of problems, one may derive amplitude equations that govern the weakly nonlinear development of an instability. Amplitude equations describe the slow modulation in space and time of disturbances excited near the threshold of an instability. The form of the amplitude equations is determined generically by symmetries of the governing equations and the structure of the linear instability ([5], [3]).

When a large, dissipative, system undergoes a Hopf bifurcation, with a trivial steady state losing stability to a growing, unsteady wave pattern, an amplitude equation that generically arises is the complex Ginzburg-Landau equation (CGL)

$$\frac{\partial A}{\partial t} = \mu A + \nu \frac{\partial^2 A}{\partial x^2} - \zeta A \left|A\right|^2 . \tag{1}$$

The function $A = A(x,t)$ is a complex valued function of two real variables. It represents the slowly varying amplitude envelope of packets of waves generated by the instability. The variable x is spatial displacement in a frame moving at the group velocity of the unstable wavepackets. The coefficients μ, ν, and ζ are complex, with $\mathbb{Re}\{\mu\} > 0$, $\mathbb{Re}\{\nu\} > 0$. When $\mathbb{Re}\{\zeta\} > 0$, the cubic nonlinearity will balance the linear growth term and halt the growth of the disturbance when $|A|$ becomes large enough. This case is a supercritical bifurcation. If $\mathbb{Re}\{\zeta\} < 0$, the cubic term will never balance the linear growth term and the equation predicts growth without bound. In such cases, the bifurcation is subcritical and equation (1) is not a good asymptotic description of the nonlinear dynamics. Higher order terms must be calculated that balance the exponential growth. Whereas μ and ν can be predicted from a knowledge of the linear theory alone, ζ and the all important sign of $\mathbb{Re}\{\zeta\}$ cannot be predicted without a nonlinear theory, and must be determined case by case by direct calculation.

To understand the origin of equation (1), consider the situations depicted in figure 6. When a system is weakly unstable, the unstable modes grow exponentially, but very slowly.

Most of the stable modes, on the other hand are relatively strongly damped. Because the stable modes decay rapidly, they are present in the system only to the extent that they are forced by nonlinear interactions with the unstable modes. Their evolution is slaved to that of the unstable modes. In many cases, Ginzburg-Landau type amplitude equations emerge from asymptotic methods that exploit the timescale separation between the stable and unstable modes.

Equation (1) governs only systems that are sufficiently large in the following sense. The spatial variations of the unstable wave packets must be produced by the interaction of a large number of closely spaced unstable modes. In a system of finite size, the spectrum of available wavenumbers must be discrete to satisfy boundary conditions. The smaller the system becomes, the larger the separation between neighboring modes in wavenumber space. If the modes are widely spaced, then a weakly unstable state may consist of only one or a small number of weakly unstable modes with all others relatively strongly damped, as shown in figure 6b. The amplitude equations governing such a situation would be a finite system of real, ordinary differential equations in time for the amplitudes of the unstable modes [2]. However, if the system is infinitely large, then the wavenumber spectrum is continuous. In that case, when the system is weakly unstable, a narrow band containing an infinite number of modes becomes unstable as shown in figure 6a. The nonlinear interaction of an infinite number of slowly evolving unstable modes leads to amplitude PDEs such as equation (1), rather than amplitude ODEs. Even when a system is finite, if it is sufficiently large that weak instability leads to the nonlinear interaction of a large number of closely spaced unstable modes, then equation (1) is still the appropriate asymptotic description of the evolution of the instability.

Though the form of equation (1) can be guessed *a priori* from considerations of symmetry [5], one must calculate the equation in detail in order to discover an expression for ζ. Knowing the coefficients is useful, and not only because the sign of $\mathbb{R}\mathsf{e}\{\zeta\}$ determines whether the Hopf bifurcation is supercritical or subcritical. Solutions of the complex Ginzburg-Landau equation exhibit a rich variety of different qualitative behaviors as the coefficients are varied. In large regions of parameter space, spatiotemporal chaos, intermittency, or the spontaneous formation of coherent structures may be observed. In others regions, stable, monochromatic plane wave solutions dominate. By computing the coefficients in terms of physical variables, it is possible to determine which of these behaviors are characteristic of the real physical system.

In this paper, we derive a complex Ginzburg-Landau equation for baroclinic instability. Baroclinic instability is important in the study of the atmosphere and oceans. It is the mechanism that generates weather systems in the midlatitude atmosphere, and it generates eddies in the oceans that are responsible for a great deal of heat transport from the equator to the poles. Baroclinic instability occurs when vertical shear flows driven by horizontal temperature gradients in a rotating domain become unstable, and large, wavelike disturbances develop that redistribute temperature fields in a kind of horizontally slanted convection.

A number of models have been used to study this phenomenon, the most well known of which are the Charney model and the Eady model. A basic introduction to these models and others can be found in the textbooks by Pedlosky [9], and Gill [4]. In this analysis, we use perhaps the simplest model exhibiting baroclinic instability. Introduced by Phillips in

1954 [10], it consists of a two-layer quasi-geostrophic flow in a rotating channel as shown in figure 1. Phillips analyzed the linear stability of a shear flow in which the fluid in each layer moves with a uniform zonal velocity. The basic state differs from that of the standard Kelvin-Helmholtz instability because rotation forces a slanting of the free surface between the two layers in order to balance the Coriolis force on the zonal flow. Phillips found that instability occurs when the difference between the velocities of the two layers exceeds a critical threshold. The model can easily be modified to include important physical effects, such as dissipation or a planetary vorticity gradient β.

The present work is motivated by a series of papers by Pedlosky ([6], [7], and a paper by Romea [11] that analyzed the nonlinear development of baroclinic instability in the Phillips model in a number of physically interesting situations. Pedlosky's papers, in particular, were the first to use multiscale asymptotic methods to compute amplitude equations for baroclinic instability. In contrast to the present effort, Pedlosky and Romea used periodic zonal boundary conditions and were therefore investigating the nonlinear interaction of a discrete spectrum of unstable modes. Consequently, their calculation led to amplitude ODEs as described above. Periodic boundary conditions are physically motivated for a model of atmospheric dynamics, because the midlatitude β-plane is typically conceived as a periodic strip wrapping around the earth. A typical wavelength for a baroclinic disturbance in the atmosphere is about 2000 km, which leaves space for only ten to fifteen wave periods in a complete traversal of the globe at midlatitudes. Nonetheless, there are physical examples of baroclinic instability to which the large aspect ratio approximation is applicable. For example, baroclinic instability produces eddies in ocean currents on the scale of 200 km. In an ocean measuring several thousand kilometers across, there is plenty of room for large scale structures to emerge. Our analysis of the large aspect ratio Phillips model should provide some insight into the kinds of structures one might expect in these situations.

To relate the CGL derived here to preexisting analysis of the qualitative behaviors of solutions of the CGL, we make use of two studies by Shraiman et al [12] and Chaté [1]. These papers present a fairly exhaustive numerical study of the parameter space of the one dimensional CGL. By mapping the coefficients calculated here onto the coefficients used in those studies, we determine what region of parameter space is inhabited by baroclinic instability. We find that most of the physical parameter space maps onto a region of CGL parameter space where non-chaotic, stable, monochromatic waves are the dominant solution at long times. Intermittent behavior may be possible when the β effect is strong compared to dissipation, but this has not been confirmed either analytically or by numerical simulation.

In §2, we give a detailed description of the Phillips Model, the physical variables involved, and the scaling limits underpinning its derivation. The physical situations examined by Pedlosky in [6], [7], and [8] are then described and contrasted with the situation considered here. In §3, the linear theory of baroclinic instability is outlined, and the CGL for baroclinic instability is derived in detail. In §4, we use the calculated coefficients to map realistic physical values of the variables onto Shraiman et al and Chaté's parameter regime, thus giving a preliminary prediction of the structures that may be observable in baroclinic instability

2 Description of the Phillips Model

The physical picture underlying the Phillips Model is given in figure 1. Two layers of fluid with different constant densities $\rho_1 < \rho_2$ lie in an infinitely long channel of finite width L and height D. The thickness of the lower layer is given by $h(x, y)$. When undisturbed, each layer has thickness $D/2$. The fluid is bounded above and below by rigid horizontal planes. The x-axis is oriented along the channel, the y-axis is oriented across the channel, and the z-axis points upward. The velocities u_1, v_1, and w_1 are the upper layer fluid velocities in the x, y, and z directions respectively. The lower layer velocities are likewise called u_2, v_2, and w_2. The pressures are given by p_1 and p_2. Each layer has viscosity ν. The gravitational acceleration is g, and the entire channel rotates with angular velocity Ω. To include the effect of the earth's sphericity, the rotation rate is assumed to vary linearly with y,

$$\Omega = \frac{1}{2}\left(f_0 + \tilde{\beta} y\right).$$

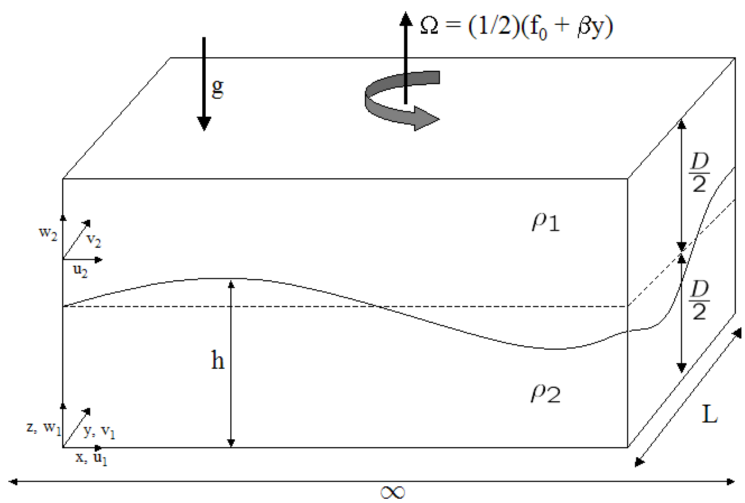

Figure 1: Physical picture of two layer channel model.

The Phillips model is derived as a scaling limit of the Navier-Stokes equations for flow in the channel. The derivation is given in greater detail in §2 of [6], but we will cover the salient points of the derivation here. Dimensionless equations of motion are obtained by scaling the dimensional variables as follows

$$(x', y') = \tfrac{(x,y)}{L}, \qquad z' = \tfrac{z}{D}, \qquad t' = \tfrac{U}{L}t,$$

$$(u_n', v_n') = \tfrac{(u_n, v_n)}{U}, \quad w_n' = \tfrac{L}{D}\tfrac{w_n}{U}, \quad h' = (h - D/2)\,\tfrac{\rho_1 U L f_0}{g(\rho_2 - \rho_1)},$$

$$p_1' = \tfrac{p_1 + \rho_1 g(z-D)}{\rho_1 U f_0 L}.$$

$$p_2' = \tfrac{p_2 + \rho_2 g(z-D/2) - \rho_1 g D/2}{\rho_2 U f_0 L}.$$

where U is a characteristic scale for the horizontal velocities. On dropping primes we find

Dimensionless Parameter	Name	Size
$\epsilon = U/(f_0 L)$,	Rossby number	$\ll 1$
$E = 2\nu/f_0 D^2$,	Ekman number	$\sim \epsilon^2$
$F = \frac{2 f_0^2 L^2}{g' D}$	rotational Froude number	O(1)
$\delta = D/L$,	cross section aspect ratio	$\ll 1$
$\beta = \tilde{\beta} L^2/U$	planetary vorticity factor	$O(1)$

Table 1: Dimensionless parameters appearing in derivation of Phillips Model.

that the dimensionless equations are

$$\begin{aligned}
\epsilon\left[\frac{\partial u_n}{\partial t} + u_n\frac{\partial u_n}{\partial x} + v_n\frac{\partial u_n}{\partial y} + w_n\frac{\partial u_n}{\partial z}\right] - (1+\epsilon\beta y)\,v_n &= -\frac{\partial p_n}{\partial x} + \frac{E}{2}\nabla_\delta^2 u_n, &(2)\\
\epsilon\left[\frac{\partial v_n}{\partial t} + u_n\frac{\partial v_n}{\partial x} + v_n\frac{\partial v_n}{\partial y} + w_n\frac{\partial v_n}{\partial z}\right] + (1+\epsilon\beta y)\,u_n &= -\frac{\partial p_n}{\partial y} + \frac{E}{2}\nabla_\delta^2 v_n, &(3)\\
\delta^2\epsilon\left[\frac{\partial w_n}{\partial t} + u_n\frac{\partial w_n}{\partial x} + v_n\frac{\partial w_n}{\partial y} + w_n\frac{\partial w_n}{\partial z}\right] &= -\frac{\partial p_n}{\partial z} + \frac{\delta^2 E}{2}\nabla_\delta^2 w_n, &(4)\\
\frac{\partial u_n}{\partial x} + \frac{\partial v_n}{\partial y} + \frac{\partial w_n}{\partial z} &= 0. &(5)
\end{aligned}$$

where

$$\nabla_\delta^2 = \frac{\partial^2}{\partial z^2} + \delta^2\left(\frac{\partial^2}{\partial x^2} + \frac{\partial^2}{\partial y^2}\right).$$

It is assumed that $\delta \ll 1$, so that horizontal straining contributes negligibly to viscous dissipation. The kinematic condition at the interface between the two layers is

$$\frac{\epsilon F}{2}\left[\frac{\partial h}{\partial t} + u_n\frac{\partial h}{\partial x} + v_n\frac{\partial h}{\partial y}\right] = w_n, \text{ at } z = \frac{1}{2}(1+\epsilon F h). \tag{6}$$

And no normal flow at the channel walls requires

$$v_n = 0, \quad \text{at} \quad y = 0, 1. \tag{7}$$

Several dimensionless parameters have appeared, all of which are defined in table 1.

The parameter F is a dimensionless measure of the width of the channel. Specifically, it compares the channel width to the distance a linear gravity wave on the interface can travel during a rotation period. The maximum speed of these waves is $c_0 = \sqrt{g'D/2}$, where $g' = g\left(\rho_2 - \rho_1\right)/\rho_2$ is the reduced gravity. The rotational period is $T = 2\pi/f_0$. Therefore,

$$F = \frac{2f_0^2L^2}{g'D} = 4\pi^2\left(\frac{L}{c_0T}\right)^2.$$

The Rossby number ϵ measures the relative importance of inertial forces and Coriolis forces. We will assume $\epsilon \ll 1$, so that the influence of rotation will be very strong. The Ekman number E measures the ratio of viscous forces to Coriolis forces, and determines the thickness of boundary layers in which viscosity plays an important role. We set $E \ll 1$ with $E^{1/2}/\epsilon = O(1)$. These limits are exploited by introducing asymptotic expansions of all the dimensionless variables in powers of ϵ, such as

$$u_n \sim u_n^{(0)} + \epsilon u_n^{(1)} + \epsilon^2 u_n^{(2)} + \cdots$$

Then, to leading order, the flow in both layers is in geostrophic and hydrostatic balance. That is,

$$u_n^{(0)} = -\tfrac{\partial p_n^{(0)}}{\partial y}, \qquad v_n^{(0)} = \tfrac{\partial p_n^{(0)}}{\partial x}, \qquad \tfrac{\partial p_n^{(0)}}{\partial z} = 0.$$

The leading order flow is also horizontally nondivergent,

$$\frac{\partial u_n^{(0)}}{\partial x} + \frac{\partial v_n^{(0)}}{\partial y} = 0,$$

which motivates the introduction of layer stream functions ψ_n such that

$$\left(u_n^{(0)}, v_n^{(0)}\right) = \hat{z} \times \nabla\psi_n.$$

By hydrostatic and geostrophic balance, the stream function is proportional to both the pressure fluctuation and the height of the interface disturbance.

Additionally, viscous forces are significant only in thin boundary layers near the top and bottom of the channel. Nevertheless, viscosity plays an important role in the dynamics of the bulk. Carefully considering the dynamics of the boundary layers, one finds that vorticity in the bulk forces forces fluid to emerge from those layers with weak vertical velocities. This phenomenon is known as Ekman pumping. These vertical velocities act to damp vorticity in the bulk through vortex stretching. From here, one may derive the evolution equations for ψ_n by manipulating the vertical vorticity equation to obtain

$$\left(\frac{\partial}{\partial t} + \frac{\partial\psi_1}{\partial x}\frac{\partial}{\partial y} - \frac{\partial\psi_1}{\partial y}\frac{\partial}{\partial x}\right)\left(\nabla^2\psi_1 + F\left(\psi_2 - \psi_1\right) + \beta y\right) = -r\nabla^2\psi_1 \tag{8}$$

$$\left(\frac{\partial}{\partial t} + \frac{\partial\psi_2}{\partial x}\frac{\partial}{\partial y} - \frac{\partial\psi_2}{\partial y}\frac{\partial}{\partial x}\right)\left(\nabla^2\psi_2 + F\left(\psi_1 - \psi_2\right) + \beta y\right) = -r\nabla^2\psi_2 \tag{9}$$

where $r = E^{1/2}\epsilon = O(1)$. In these equations, fast gravity waves have been filtered out and only the slow, vortical dynamics remain.

To investigate baroclinic instability, we write down evolution equations for perturbations from a shear solution where the velocity of the upper layer is U and the velocity of the lower layer is $-U$. Let

$$\psi_1 = -Uy + \psi_1', \qquad \psi_2 = Uy + \psi_2'.$$

and substitute into equations (8) and (9). Dropping primes, we find

$$\begin{aligned}
\left(\frac{\partial}{\partial t} + U\frac{\partial}{\partial x}\right) q_1 + \frac{\partial \psi_1}{\partial x}\left(\beta + 2FU\right) + r\nabla^2\psi_1 &= -J\left(\psi_1, q_1\right), && (10)\\
\left(\frac{\partial}{\partial t} - U\frac{\partial}{\partial x}\right) q_2 + \frac{\partial \psi_2}{\partial x}\left(\beta - 2FU\right) + r\nabla^2\psi_2 &= -J\left(\psi_2, q_2\right),, && (11)\\
q_1 &= \nabla^2\psi_1 + F\left(\psi_2 - \psi_1\right), && (12)\\
q_2 &= \nabla^2\psi_2 + F\left(\psi_1 - \psi_2\right). && (13)
\end{aligned}$$

with boundary conditions

$$\frac{\partial \psi_n}{\partial x} = 0, \qquad y = 0, 1.$$

These equations are the Phillips model of baroclinic instability.

Pedlosky and Romea's papers worked with these equations for a the channel periodic in x. In [6], Pedlosky derived amplitude ODEs for the purely viscous case $\beta = 0$ and $r = O(1)$, and the inviscid cases with $r = 0$ and $\beta = O(1)$ or $\beta = 0$. Pedlosky obtained a Ginzburg-Landau ODE with real coefficients for $\beta = 0$, $r = O(1)$. However, the small viscosity cases do not lead to Ginzburg-Landau type amplitude equations, because there is no scale separation between the decay rate of the stable modes and the growth rate of the unstable modes. Also, the case of $0 < r \ll 1$ is a singular limit of the linear theory. The introduction of an infinitesimal viscosity actually *destabilizes* the flow, reducing the critical value of U by an $O(1)$ amount. Pedlosky derived amplitude equations for this subtle case with $\beta = 0$ in [7]. In [11], Romea tackled the small r case with $\beta = O(1)$.

It seems, however, that the case with both $\beta = O(1)$ and $r = O(1)$ has never been addressed. It is interesting to know how these two effects compete when they are of comparable strength. The infinite-size limit, which introduces the possibility of spatio-temporal disorder and localized structures, has also never been investigated.

3 Derivation of CGL

The Phillips model equations (10)-(13) may be written in the form

$$\begin{aligned}
\frac{\partial}{\partial t}\mathsf{M}\Psi &= \mathsf{L}\Psi - J\left(\Psi, \mathsf{M}\Psi\right), && (14)\\
\frac{\partial \Psi}{\partial x} &= 0, \quad \text{for} \quad y = 0, 1. && (15)
\end{aligned}$$

where

$$
\begin{aligned}
\Psi &= \begin{pmatrix} \psi_1 \\ \psi_2 \end{pmatrix} \\
\mathsf{M} &= \begin{bmatrix} \nabla^2 - F & F \\ F & \nabla^2 - F \end{bmatrix} \\
\mathsf{L} &= \begin{bmatrix} -U\frac{\partial}{\partial x}\left(\nabla^2 - F\right) - (\beta + 2FU)\frac{\partial}{\partial x} - r\nabla^2 & -UF\frac{\partial}{\partial x} \\ UF\frac{\partial}{\partial x} & U\frac{\partial}{\partial x}\left(\nabla^2 - F\right) - (\beta - 2FU)\frac{\partial}{\partial x} - r\nabla^2 \end{bmatrix}
\end{aligned}
$$

and

$$
J(A, B) = \frac{\partial A}{\partial x} \star \frac{\partial B}{\partial y} - \frac{\partial A}{\partial y} \star \frac{\partial B}{\partial x}.
$$

The $\star$ operator is termwise multiplication of vectors without summing. That is

$$
\begin{pmatrix} a_1 \\ a_2 \end{pmatrix} \star \begin{pmatrix} b_1 \\ b_2 \end{pmatrix} = \begin{pmatrix} a_1 b_1 \\ a_2 b_2 \end{pmatrix}.
$$

3.1 Linear Theory

Much of the structure of the finite amplitude evolution equations is determined by the linear instability properties of the system. The linearized equations are

$$
\begin{aligned}
\frac{\partial}{\partial t}\mathsf{M}\Psi &= \mathsf{L}\Psi, \\
\frac{\partial \Psi}{\partial x} &= 0, \quad \text{for} \quad y = 0, 1.
\end{aligned} \tag{16}
$$

One may seek normal mode solutions of the form

$$
\Psi(x, y, t) = \mathbb{R}\mathsf{e}\left\{\hat{\Psi}(k, m, U) e^{\,i(kx + my - \omega t)}\right\}.
$$

Substitution of this form into equation (16) yields a system of algebraic equations

$$
\left(\hat{\mathsf{L}} + i\omega\hat{\mathsf{M}}\right)\hat{\Psi} = 0 \tag{17}
$$

where

$$
\begin{aligned}
\hat{\mathsf{M}}(k, m) &= \begin{bmatrix} -(k^2 + m^2 + F) & F \\ F & -(k^2 + m^2 + F) \end{bmatrix} \\
\hat{\mathsf{L}}(k, m, U) &= \begin{bmatrix} Uik\left(k^2 + m^2 + F\right) + \cdots \\ \quad + r\left(k^2 + m^2\right) - ik(\beta + 2FU) & -ikUF \\ & -ikU\left(k^2 + m^2 + F\right) - \cdots \\ ikUF & -ik(\beta - 2FU) + r\left(k^2 + m^2\right) \end{bmatrix}
\end{aligned}
$$

For a null vector $\hat{\Psi}$ to exist,

$$
\det\left(\hat{\mathsf{L}} + i\omega\hat{\mathsf{M}}\right) = 0 \tag{18}
$$

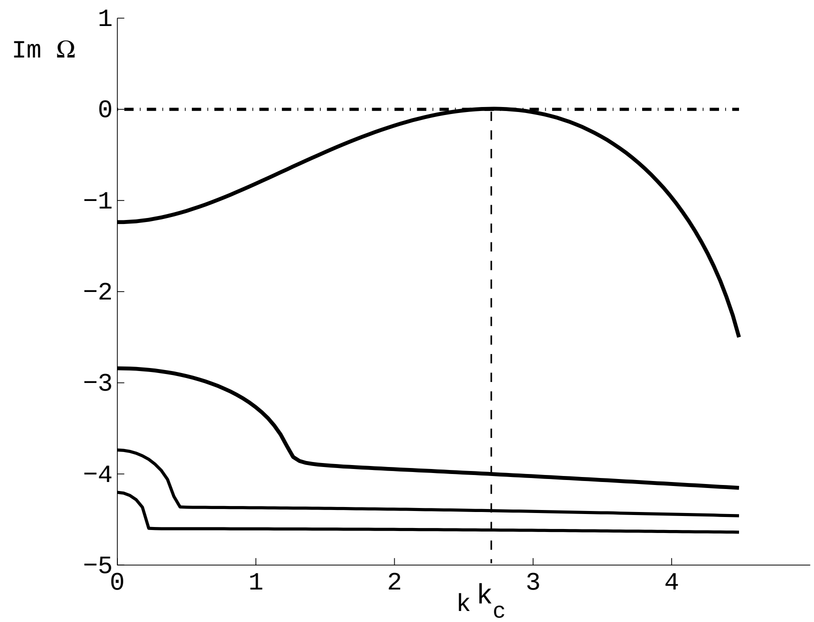

Figure 2: Growth rate curves for $m = \pi, 2\pi, 3\pi, 4\pi$, calculated for the critical shear $U = U_c$ at which a single mode $k = k_c$ is marginally stable.

must hold. Equation (18) implies that ω must be a root of a second order polynomial with coefficients that are functions of k, m, and the physical parameters of the system. Thus, for fixed values of these arguments there are at most two distinct values of ω satisfying equation (18). This condition defines the dispersion relationships

$$\begin{aligned} \omega &= \Omega\left(k, m, U, d\right) \\ &= -\left(\frac{\beta k}{K^2} + ir\right)\frac{\left(K^2+F\right)}{\left(K^2+2F\right)} + (-1)^d\,\frac{\sqrt{k^2K^4\left(K^4-4F^2\right)U^2+F^2\left(\beta k+irK^2\right)^2}}{K^2\left(K^2+2F\right)} \end{aligned} \tag{19}$$

where $d = 1, 2$, and $K^2 = k^2 + m^2$. A mode is stable if $\mathbb{Im}\left\{\Omega\right\} < 0$ and unstable if $\mathbb{Im}\left\{\Omega\right\} > 0$.

Because of the boundary condition (15), normal mode solutions exist only for $m = \pi, 2\pi, 3\pi, \ldots$ when $k \neq 0$. However, because the channel is infinite in the x direction there is a continuous spectrum of solutions in k. Plotting $\mathbb{Im}\left\{\Omega\right\}$ for admissible k and m produces a discrete set of growth rate curves, as shown in figure (2).

When all the growth rate curves lie in $\mathbb{Im}\left\{\Omega\right\} < 0$, the system is stable to infinitesimal perturbations. For fixed (k, m), one may compute the critical value of the shear $U = U_{\mathrm{marg}}(k, m)$ at which that particular mode becomes marginally stable by setting $\mathbb{Im}\left\{\Omega(k, m, U, d)\right\} = 0$ and solving for U. One may use the identity

$$\mathbb{Re}\left\{\sqrt{a+bi}\right\} = \mathrm{sgn}(a)\sqrt{\frac{1}{2}\sqrt{a^2+b^2}+\frac{1}{2}a}$$

and perform some lengthy algebra, the result of which is

$$U_{\text{marg}}(k,m) = \sqrt{\frac{\left(\frac{r}{k}\right)^2 K^4 \left(K^2+F\right)^2 + F^2\beta^2}{K^2\left(K^2+F\right)^2\left(2F-K^2\right)}} \tag{20}$$

The mode is stable for $U < U_{\text{marg}}(k,m)$. Therefore, the entire system is stable for

$$U < U_c = \inf_{\substack{0 \le K^2 \le 2F \\ m=n\pi}} U_{\text{marg}}(k,m) \tag{21}$$

It is worth noting that equation (20) implies that instability is impossible for $F < \pi^2/2$. Furthermore, one can show that U_{marg} increases monotonically with m, so that the first modes to become marginally stable as U is increased will lie on the $m = \pi$ curve.

3.2 Nonlinear modulation

At $U = U_c$, a single mode (k_c, π) has $\mathbb{Im}\{\Omega(k_c,\pi)\} = 0$, and all other modes are stable. The purpose of this work is to learn what happens when the shear is increased slightly above U_c and the system becomes weakly unstable. As the modes grow, their nonlinear interactions play a pivotal role in the subsequent evolution of the instability.

Figure (6) visually summarizes the insight into this situation that linear theory provides. If $U = U_c + \Delta$, with $|\Delta| \ll 1$, then the maximum growth rate is positive and $O(|\Delta|)$. The growth rate curve is well described by a parabolic function in the neighborhood of its maximum, so there is a band of unstable wavenumbers of width $O\left(|\Delta|^{1/2}\right)$ around $k = k_c$.

Any exact solution to (14), (15) can be written in the form

$$\Psi(x,y,t) = \sum_{n=1}^{\infty}\int_{-\infty}^{\infty} A_{k,n\pi}(t)\hat{\Psi}(k,n\pi,U)e^{i[kx+n\pi y-\Omega(k,n\pi,U)t]}\,dk \tag{22}$$

Here, $\hat{\Psi}(k,m,U)$ is the mode eigenvector defined by equation (17), and $A_{k,m}(t)$ tracks the time evolution of the amplitude of mode (k,m). The amplitudes of the unstable modes will dominate because, as mentioned above, strongly stable modes decay rapidly and are present due only to nonlinear forcing by the slowly evolving stable modes. That is, $A_{k,m}$ should be strongly peaked near $k = k_c$ on the $m = \pi$ branch.

Using this assumption to write an approximate form for the Fourier series-transform solution (22) will motivate scalings for an asymptotic solution of this problem. First, neglecting the summands for $n \neq 1$ and changing the integration variable to center on $k = k_c$ gives

$$\Psi(x,y,t) \approx \int_{-\infty}^{\infty} A_{k_c+k',\pi}(t)\hat{\Psi}(k_c+k',\pi)e^{(i((k_c+k')x+\pi y-\Omega(k_c+k',\pi,U_c+\Delta)t))}dk'$$

Now, we make use of the fact that the dominant contribution to the integral comes from $k' = O\left(|\Delta|^{1/2}\right)$. Let $\tilde{k} = |\Delta|^{-1/2}k'$ and Taylor expand the integrand about k_c. One finds:

$$\Psi(x,y,t) \approx \hat{\Psi}(k_c,\pi)e^{i(k_c x+\pi y-\Omega(k_c,\pi,U_c)t)}\int_{-\infty}^{\infty}\tilde{A}_{\tilde{k}}(t)e^{i|\Delta|^{1/2}\tilde{k}\left(x-\frac{\partial\Omega}{\partial k}\big|_{k=k_c}t\right)-i\Delta\frac{\partial\Omega}{\partial U}\big|_{U=U_c}t}d\tilde{k}$$

where $\tilde{A}_{\tilde{k}} = |\Delta|^{1/2} A_{k_c+|\Delta|^{1/2}\tilde{k}}(t)$. This expression is the product of the marginally stable mode at criticality with an amplitude envelope slowly varying in space and time:

$$\Psi(x,y,t) \approx A\left(|\Delta|^{1/2}(x-c_g t), |\Delta|\, t\right) \hat{\Psi}(k_c, \pi, U_c) e^{(i(k_c x + \pi y - \Omega_c t))}. \tag{23}$$

Here,

$$c_g = \left.\frac{\partial \Omega}{\partial k}\right|_{k=k_c} \tag{24}$$

is the group velocity of the marginally unstable mode. We also write $\Omega_c = \Omega(k_c, \pi, U_c)$ and $\hat{\Psi}_c = \hat{\Psi}(k_c, \pi, U_c)$.

Note that there is only one marginal wave at criticality, and not a pair of waves traveling in opposite directions. This fact can be established by noting that, though the critical branch satisfies $\mathbb{Im}\{\Omega\} = 0$ for both k_c and $-k_c$, we have $\mathbb{Re}\{\Omega(-k_c, \pi, 1)\} = -\mathbb{Re}\{\Omega(k_c, \pi, 1)\}$. This implies that the critical modes (k_c, π) and $(-k_c, \pi)$ differ by only a phase shift. The second branch associated with (k_c, π) is strongly damped. This loss of symmetry is due to the β-effect, which imposes a directionality to the propagation of waves supported by the planetary vorticity gradient.

3.3 Method of Multiple Scales

The considerations leading to equation (23) reveal the proper scalings to use in a multiple-scales approach to this problem. Let

$$U = U_c + \Delta, \quad T = |\Delta|^{1/2}\, t, \quad \tau = |\Delta|\, t, \quad X = |\Delta|^{1/2}\, x.$$

Then, seek a solution for Ψ of the form

$$\Psi = |\Delta|^{1/2}\, \Psi^{(1)}(t,x,y,T,\tau,X) + |\Delta|\, \Psi^{(2)}(t,x,y,T,\tau,X) + |\Delta|^{3/2}\, \Psi^{(3)}(t,x,y,T,\tau,X) + \cdots$$

The introduction of new space and time scales requires, by the chain rule,

$$\begin{aligned}
\frac{\partial}{\partial t} &\rightarrow \frac{\partial}{\partial t} + |\Delta|^{1/2}\frac{\partial}{\partial T} + |\Delta|\frac{\partial}{\partial \tau}, \\
\frac{\partial}{\partial x} &\rightarrow \frac{\partial}{\partial x} + |\Delta|^{1/2}\frac{\partial}{\partial X}, \\
\nabla^2 &\rightarrow \nabla^2 + 2\,|\Delta|^{1/2}\frac{\partial^2}{\partial x \partial X} + |\Delta|\frac{\partial^2}{\partial X^2}.
\end{aligned}$$

Substituting these transformations into the system (14), (15) and collecting terms of like order in $|\Delta|$, one may obtain a hierarchy of inhomogeneous linear problems. The most straightforward way of doing this requires the explicit manipulation of the terms of M and L. Unfortunately, proceeding in this manner produces extremely messy algebra and complicated expressions that are difficult to interpret in terms of physical properties of the system. However, it is possible to develop the expansion in general terms without considering the detailed structure of the operators M and L. By keeping track of only the formal structure of the expansion, we will be able to make useful simplifications throughout the computation.

When the linear operators M and L are applied to slowly varying wave packets, they can be expanded in the following way. First, note that

$$\mathsf{M}\left(\partial_x + |\Delta|^{1/2}\,\partial_X, \partial_y\right) A(X,T,\tau)\hat{\Psi}(k,m)e^{i(kx+my)} = \hat{\mathsf{M}}\left(k - i\,|\Delta|^{1/2}\frac{\partial}{\partial X}, m\right) A\hat{\Psi}e^{i(kx+my)}.$$

Formally, we may treat ∂_X as a variable and Taylor expand $\hat{\mathsf{M}}$ to find

$$\begin{aligned}\mathsf{M}\left(\partial_x + |\Delta|^{1/2}\,\partial_X, \partial_y\right) A\hat{\Psi}e^{i(kx+my)} \;=\; & \left[\hat{\mathsf{M}}(k,m) - i\,|\Delta|^{1/2}\frac{\partial\hat{\mathsf{M}}}{\partial k}(k,m)\frac{\partial}{\partial X}\right. \\ & \left. -\frac{|\Delta|}{2}\frac{\partial^2\hat{\mathsf{M}}}{\partial k^2}(k,m)\frac{\partial^2}{\partial X^2} + \cdots\right] A\hat{\Psi}e^{i(kx+my)}.\end{aligned}$$

Thus, the formal expansion of M takes the form

$$\begin{aligned}\mathsf{M}A(X,T,\tau)\hat{\Psi}(k,m,U)e^{\,i(kx+my-\Omega t)} \;\to\; & \left[A\hat{\mathsf{M}}\hat{\Psi} - |\Delta|^{1/2}\frac{\partial A}{\partial X}\left(i\frac{\partial\hat{\mathsf{M}}}{\partial k}\hat{\Psi}\right)\right. \\ & \left. -\frac{|\Delta|}{2}\frac{\partial^2 A}{\partial X^2}\left(\frac{\partial^2\hat{\mathsf{M}}}{\partial k^2}\hat{\Psi}\right) + \cdots\right] e^{i(kx+my-\Omega t)}.\end{aligned}$$

Likewise, the formal expansion of L takes the form

$$\begin{aligned}\mathsf{L}A(X,T,\tau)\hat{\Psi}(k,m,U)e^{\,i(kx+my-\Omega t)} \;\to\; & e^{\,i(kx+my-\Omega t)}\left[A\hat{\mathsf{L}}\hat{\Psi} - |\Delta|^{1/2}\frac{\partial A}{\partial X}\left(i\frac{\partial\hat{\mathsf{L}}}{\partial k}\hat{\Psi}\right)\right. \\ & \left. +|\Delta|\left(\mathrm{sgn}(\Delta)A\frac{\partial\hat{\mathsf{L}}}{\partial U}\hat{\Psi} - \frac{1}{2}\frac{\partial^2 A}{\partial X^2}\left(\frac{\partial^2\hat{\mathsf{L}}}{\partial k^2}\hat{\Psi}\right)\right)\right].\end{aligned}$$

To simplify notation, let $\hat{\mathsf{L}}_o = \hat{\mathsf{L}}(k_c,\pi,U_c)$ and $\hat{\mathsf{M}}_o = \hat{\mathsf{M}}(k_c,\pi)$.

Utilizing these expansions and collecting terms of $O\left(|\Delta|^{1/2}\right)$ yields the leading order problem

$$\begin{aligned}\left(\frac{\partial}{\partial t}\mathsf{M}_o - \mathsf{L}_o\right)\Psi^{(1)} &= 0, & (25)\\ \frac{\partial\Psi^{(1)}}{\partial x} &= 0, \quad \text{for} \quad y = 0,1. & (26)\end{aligned}$$

This is the linear problem (16) at the marginal shear U_c. There are infinitely many normal mode solutions, but all will decay at long times $T = O(1)$ except for the marginally stable mode. As we are concerned with the long time evolution of the instability, we take the leading order solution to be

$$\Psi^{(1)} = \mathbb{R}\mathsf{e}\left\{A(X,T,\tau)\hat{\Psi}_c e^{i(k_c x - \Omega_c t)}\sin\pi y\right\}. \tag{27}$$

Collecting terms of $O\left(|\Delta|\right)$ yields

$$\begin{aligned}\left(\frac{\partial}{\partial t}\mathsf{M}_o - \mathsf{L}_o\right)\Psi^{(2)} &= -\frac{\partial}{\partial T}\hat{\mathsf{M}}_o\Psi^{(1)} + i\frac{\partial}{\partial t}\frac{\partial\hat{\mathsf{M}}}{\partial k}\frac{\partial\Psi^{(1)}}{\partial X} - i\frac{\partial\hat{\mathsf{L}}}{\partial k}\frac{\partial\Psi^{(1)}}{\partial X} - J\left(\Psi^{(1)}, \hat{\mathsf{M}}_0\Psi^{(1)}\right), \\ \frac{\partial\Psi^{(2)}}{\partial x} &= 0, \quad \text{for} \quad y = 0, 1. \end{aligned} \tag{28}$$

The operator on the left hand side of this equation is the same as in equation (26). Thus, inhomogeneous terms proportional to the marginally stable mode will produce a secular response in $\Psi^{(2)}$. The elimination of these secular terms introduces a first constraint on the evolution of $A(X, T, \tau)$.

Substituting the solution (27) into equation (28), one finds

$$\begin{aligned}\left(\frac{\partial}{\partial t}\mathsf{M}_o - \mathsf{L}_o\right)\Psi^{(2)} &= \mathbb{R}\mathsf{e}\left\{\left(-\hat{\mathsf{M}}_o\hat{\Psi}_c\frac{\partial A}{\partial T} - i\left[\frac{\partial\hat{\mathsf{L}}}{\partial k} + i\Omega_c\frac{\partial\hat{\mathsf{M}}}{\partial k}\right]\hat{\Psi}_c\frac{\partial A}{\partial X}\right)e^{\,i(k_c x - \Omega_c t)}\right\}\sin\pi y \\ &\quad + \mathbb{I}\mathsf{m}\left\{\hat{\Psi}_c \star \overline{\hat{\mathsf{M}}_o\hat{\Psi}_c}\right\}\frac{\pi k_c}{2}|A|^2\sin 2\pi y. \end{aligned} \tag{29}$$

The overbar represents complex conjugation. Since equation (29) is linear, $\Psi^{(2)}$ takes the form

$$\Psi^{(2)} = \mathbb{R}\mathsf{e}\left\{A^{(2)}(X, T, \tau)e^{\,i(k_c x - \Omega_c t)}\right\}\sin\pi y + B^{(2)}(X, T, \tau)\sin 2\pi y + U^{(2)}(X, T, \tau)\left(y - \frac{1}{2}\right).$$

The first term represents a correction proportional to the marginally stable mode. The second two terms are independent of x, and represent an $O(|\Delta|)$ correction to the zonal mean flow. Substituting this form into equation (29) and collecting terms proportional to $\sin 2\pi y$ yields a problem for $B^{(2)}$:

$$-\hat{\mathsf{L}}(0, 2\pi, U_c)B^{(2)} = \frac{k_c\pi}{2}\mathbb{I}\mathsf{m}\left\{\hat{\Psi}_c \star \overline{\hat{\mathsf{M}}_o\hat{\Psi}_c}\right\}|A|^2$$

Using

$$\hat{\mathsf{L}}(0, 2\pi, U_c) = 4\pi^2 r\mathsf{I}$$

gives

$$B^{(2)} = -\frac{k_c}{8\pi r}\mathbb{I}\mathsf{m}\left\{\hat{\Psi}_c \star \overline{\hat{\mathsf{M}}_o\hat{\Psi}_c}\right\}|A|^2. \tag{30}$$

Collecting terms proportional to $\sin\pi y$ yields a problem for $A^{(2)}$:

$$\left(\hat{\mathsf{L}}_o + i\Omega_c\hat{\mathsf{M}}_o\right)A^{(2)} = \hat{\mathsf{M}}_o\hat{\Psi}_c\frac{\partial A}{\partial T} + i\left(\frac{\partial\hat{\mathsf{L}}}{\partial k} + i\Omega_c\frac{\partial\hat{\mathsf{M}}}{\partial k}\right)\hat{\Psi}_c\frac{\partial A}{\partial X}$$

Now, as demonstrated by equation (17), the operator on the left hand side is singular. For the equation to be solvable, the right hand side must be orthogonal to the operator's left null vector. That is, for $\hat{\Psi}_c^{\dagger}$ such that

$$\hat{\Psi}_c^{\dagger}\left(\hat{\mathsf{L}}_o + i\Omega_c\hat{\mathsf{M}}_o\right) = 0,$$

we must have

$$\hat{\Psi}_c^\dagger \left[\hat{\mathsf{M}}_o \hat{\Psi}_c \frac{\partial A}{\partial T} + i\left(\frac{\partial \hat{\mathsf{L}}}{\partial k} + i\Omega_c \frac{\partial \hat{\mathsf{M}}}{\partial k}\right) \hat{\Psi}_c \frac{\partial A}{\partial X}\right] = 0. \tag{31}$$

This equation implies something about the evolution of A. Unfortunately, it is a mess and difficult to interpret physically, especially if the matrix products are written out in full. It is at this point that our attention to the formal structure of the expansion becomes useful. Note that

$$\frac{\partial}{\partial k}\left[\left(\hat{\mathsf{L}}_o + i\Omega(k,\pi,U_c)\right)\hat{\Psi}\left(k,\pi,U_c\right)\right] = 0.$$

If we expand this expression with the product rule and evaluate at $k = k_c$, we find

$$\left(\frac{\partial \hat{\mathsf{L}}}{\partial k} + i\Omega_c \frac{\partial \hat{\mathsf{M}}}{\partial k}\right)\hat{\Psi}_c = -i\left.\frac{\partial \Omega}{\partial k}\right|_{k=k_c} \hat{\mathsf{M}}_o \hat{\Psi}_c - \left(\hat{\mathsf{L}}_o + i\Omega_c \hat{\mathsf{M}}_o\right)\frac{\partial \hat{\Psi}}{\partial k}.$$

That is, the operator splits into a term proportional to the group velocity of the marginal wave (see equation (24)) and a term that is orthogonal to the left null vector $\hat{\Psi}_c^\dagger$ by definition! Substituting this new relation into equation (31) yields a more familiar evolution equation for A:

$$\frac{\partial A}{\partial T} + c_g \frac{\partial A}{\partial X} = 0.$$

The amplitude envelope propagates at the group velocity of the marginally stable wave. We now write $A(X,T,\tau) = A(\eta,\tau)$ where $\eta = X - c_g T$. We also have

$$\frac{\partial}{\partial X} = \frac{\partial}{\partial \eta}, \qquad \frac{\partial}{\partial T} = -c_g \frac{\partial}{\partial \eta}.$$

It is still necessary to solve for $A^{(2)}$. One solution is

$$A^{(2)} = -i\frac{\partial \hat{\Psi}}{\partial k}\frac{\partial A}{\partial \eta}. \tag{32}$$

One might add a homogeneous term proportional to $\hat{\Psi}_c$ to this solution, but the inclusion of such a term has no impact on the results of the computation. The term is proportional to $\Psi^{(1)}$, so we may simply require that it be absorbed into the leading order solution.

Finally, $U^{(2)}$ is determined by enforcing the boundary condition (15). It can be shown [10] that the normal flow condition implies a constraint on the zonally averaged flow at the boundaries,

$$\frac{\partial}{\partial t}\overline{u_n} = \lim_{M\to\infty}\frac{1}{2M}\int_{-M}^{M}\frac{\partial^2 \psi_n}{\partial y \partial t}dx = 0, \qquad \text{for } y = 0, 1.$$

This equation implies that, as higher order corrections develop, they cannot alter the mean zonal flow at the boundaries. We deduce that,

$$U^{(2)} = -2\pi B^{(2)}$$

To summarize, we have found

$$\Psi^{(2)} = \mathbb{R}\mathsf{e}\left\{-i\frac{\partial \hat{\Psi}}{\partial k}\frac{\partial A}{\partial \eta}e^{i(k_c x - \Omega_c t)}\right\}\sin \pi y - \frac{k_c}{8\pi r}\mathbb{I}\mathsf{m}\left\{\hat{\Psi}_c \star \overline{\hat{\mathsf{M}}_o \hat{\Psi}_c}\right\}|A|^2\left(\sin 2\pi y - 2\pi\left(y - \frac{1}{2}\right)\right).$$

Collecting terms of $O\left(|\Delta|^{3/2}\right)$ yields

$$\begin{aligned}
\left(\frac{\partial}{\partial t}\mathsf{M}_o-\mathsf{L}_o\right)\Psi^{(3)} \quad = \quad & -\left(\frac{\partial}{\partial T}\hat{\mathsf{M}}_o+i\left(\frac{\partial\hat{\mathsf{L}}}{\partial k}-\frac{\partial}{\partial t}\frac{\partial\hat{\mathsf{M}}}{\partial k}\right)\frac{\partial}{\partial X}\right)\Psi^{(2)} \\
& -\left(\frac{\partial}{\partial\tau}\hat{\mathsf{M}}_o-i\frac{\partial^2}{\partial X\partial T}\frac{\partial\hat{\mathsf{M}}}{\partial k}+\frac{1}{2}\frac{\partial^2}{\partial X^2}\left(\frac{\partial^2\hat{\mathsf{L}}}{\partial k^2}-\frac{\partial}{\partial t}\frac{\partial^2\hat{\mathsf{M}}}{\partial k^2}\right)+\Delta\frac{\partial\hat{\mathsf{L}}}{\partial U}\right)\Psi^{(1)} \\
& -J\left(\Psi^{(2)},\hat{\mathsf{M}}_o\Psi^{(1)}\right)-J\left(\Psi^{(1)},\hat{\mathsf{M}}_o\Psi^{(2)}\right)+\tilde{J}\left(\Psi^{(1)},\hat{\mathsf{M}}\Psi^{(1)}\right). \qquad (33)
\end{aligned}$$

where

$$\tilde{J}\left(\Psi^{(1)},\hat{\mathsf{M}}\Psi^{(1)}\right)=\frac{\partial\Psi^{(1)}}{\partial X}\frac{\partial}{\partial y}\left(\hat{\mathsf{M}}_o\Psi^{(1)}\right)-\frac{\partial\Psi^{(1)}}{\partial y}\frac{\partial}{\partial X}\left(\hat{\mathsf{M}}_o\Psi^{(1)}\right).$$

Since our only purpose in proceeding to this order is to find another evolution equation for A, it is not necessary to solve for $\Psi^{(3)}$ in full. We simply note that the right hand side of equation (33) contains terms proportional to $e^{\,i(k_cx-\Omega_ct)}\sin\pi y$, $\sin 2\pi y$, and $e^{\,i(k_cx-\Omega_ct)}\sin 3\pi y$. Therefore, since the problem is linear we may assume

$$\Psi^{(3)}=\mathbb{R}\mathsf{e}\left\{e^{\,i(k_cx-\Omega_ct)}\left(A^{(3)}\sin\pi y+B^{(3)}\sin 3\pi y\right)\right\}+C^{(3)}\sin 2\pi y-U^{(3)}y.$$

The evolution equation we seek will emerge as we attempt to solve for $A^{(3)}$. Substituting in the solutions for $\Psi^{(1)}$ and $\Psi^{(2)}$ and equating terms proportional to $\sin\pi y$ yields

$$\left(\hat{\mathsf{L}}_o+i\Omega_c\hat{\mathsf{M}}\right)A^{(3)}=\left(\hat{\mathsf{M}}_o\hat{\Psi}_c\right)\frac{\partial A}{\partial\tau}-\left(\frac{\Delta}{|\Delta|}\frac{\partial\hat{\mathsf{L}}}{\partial U}\hat{\Psi}_c\right)A+\Pi_1\frac{\partial^2A}{\partial\eta^2}+\Pi_2A\,|A|^2. \qquad (34)$$

where

$$\Pi_1=\frac{1}{2}\left[\left(\frac{\partial^2\hat{\mathsf{L}}}{\partial k^2}+i\Omega_c\frac{\partial^2\hat{\mathsf{M}}}{\partial k^2}\right)\hat{\Psi}_c+2\left(\frac{\partial\hat{\mathsf{L}}}{\partial k}+i\Omega_c\frac{\partial\hat{\mathsf{M}}}{\partial k}\right)\frac{\partial\hat{\Psi}}{\partial k}+2i\frac{\partial\Omega}{\partial k}\frac{\partial}{\partial k}\left(\hat{\mathsf{M}}_o\hat{\Psi}_c\right)\right],$$

and

$$\Pi_2=-\frac{ik_c^2}{8r}\left[3\mathbb{I}\mathsf{m}\left\{\hat{\Psi}_c\star\overline{\hat{\mathsf{M}}_o\hat{\Psi}_c}\right\}\star\left(\hat{\mathsf{M}}_o\hat{\Psi}_c\right)-\mathcal{M}\mathbb{I}\mathsf{m}\left\{\hat{\Psi}_c\star\overline{\hat{\mathsf{M}}_o\hat{\Psi}_c}\right\}\star\hat{\Psi}_c\right],$$

where

$$\mathcal{M}=\hat{\mathsf{M}}\left(0,2\pi\right)+\begin{pmatrix}-2F & 2F\\ 2F & -2F\end{pmatrix}=\begin{pmatrix}-4\pi^2-3F & 3F\\ 3F & -4\pi^2-3F\end{pmatrix}.$$

Using the relationship

$$\frac{\partial^2}{\partial k^2}\left[\left(\hat{\mathsf{L}}_o+i\Omega(k,\pi,U_c)\right)\hat{\Psi}\left(k,\pi,U_c\right)\right]=0,$$

one can show that

$$\Pi_1=-\frac{1}{2}i\frac{\partial^2\Omega}{\partial k^2}\hat{\mathsf{M}}_o\hat{\Psi}_c-\left(\hat{\mathsf{L}}_o+i\Omega_c\hat{\mathsf{M}}_o\right)\frac{\partial^2\hat{\Psi}}{\partial k^2}.$$

Likewise, using

$$\frac{\partial}{\partial U}\left[\left(\hat{\mathsf{L}}_o+i\Omega(k,\pi,U_c)\right)\hat{\Psi}\left(k_c,\pi,U\right)\right]=0,$$

one may show that

$$\frac{\partial\hat{\mathsf{L}}}{\partial U}\hat{\Psi}_c = -i\frac{\partial\Omega}{\partial U}\hat{\mathsf{M}}_o\hat{\Psi}_c - \left(\hat{\mathsf{L}}_o + i\Omega_c\hat{\mathsf{M}}_o\right)\frac{\partial\hat{\Psi}}{\partial U}.$$

Finally, forming the solvability condition as in equation (31) gives

$$\frac{\partial A}{\partial\tau} = \mu A + \nu\frac{\partial^2 A}{\partial\eta^2} - \zeta A\left|A\right|^2. \tag{35}$$

where the coefficients are given by

$$\mu = \operatorname{sgn}(\Delta)\frac{\hat{\Psi}_c^\dagger\frac{\partial\hat{\mathsf{L}}}{\partial U}\hat{\Psi}_c}{\hat{\Psi}_c^\dagger\hat{\mathsf{M}}_o\hat{\Psi}_c} = -i\operatorname{sgn}(\Delta)\left.\frac{\partial\Omega}{\partial U}\right|_{k=k_c}, \tag{36}$$

$$\nu = \frac{1}{2}i\left.\frac{\partial^2\Omega}{\partial k^2}\right|_{k=k_c} \tag{37}$$

$$\zeta = \frac{ik_c^2}{8r}\frac{\hat{\Psi}_c^\dagger\left(3\mathbb{I}\mathsf{m}\left\{\hat{\Psi}_c\star\overline{\hat{\mathsf{M}}_o\hat{\Psi}_c}\right\}\star\left(\hat{\mathsf{M}}_o\hat{\Psi}_c\right) - \mathcal{M}\mathbb{I}\mathsf{m}\left\{\hat{\Psi}_c\star\overline{\hat{\mathsf{M}}_o\hat{\Psi}_c}\right\}\star\hat{\Psi}_c\right)}{\hat{\Psi}_c^\dagger\hat{\mathsf{M}}_o\hat{\Psi}_c}. \tag{38}$$

We have derived a complex Ginzburg-Landau equation governing the onset of baroclinic instability in a two layer model. The expressions for the coefficients are expressed in terms of quantities computable from the linear theory of baroclinic modes. Specifically, we have

$$\hat{\Psi}_c = (1,\gamma)^T,$$

where

$$\gamma = \frac{K_c^2+F}{F} - \frac{\beta+2FU_c}{F\left(U_c-c\right)} - i\frac{r}{k_c}\frac{K_c^2}{F\left(U_c-c\right)}.$$

where $c = \Omega_c/k_c$. A useful fact about γ is that

$$\gamma^{-1} = \frac{K_c^2+F}{F} + \frac{\beta-2FU_c}{F\left(U_c+c\right)} + i\frac{r}{k_c}\frac{K_c^2}{F\left(U_c+c\right)}.$$

The left null vector $\hat{\Psi}_c^\dagger$ is simply

$$\hat{\Psi}_c^\dagger = \left(1, -\frac{U_c-c}{U_c+c}\gamma\right).$$

After some algebra, one finds the following explicit expressions for the coefficients:

$$\mu = \frac{ik_cF\operatorname{sgn}(\Delta)\left[\frac{1+\gamma}{U_c-c} + \frac{\gamma+\gamma^2}{U_c+c} - \frac{K_c^2}{F(U_c-c)} - \frac{\gamma^2K_c^2}{F(U_c+c)}\right]}{Z+\gamma^2Z'}, \tag{39}$$

$$\begin{aligned}\nu = \frac{1}{Z+\gamma^2Z'}\Bigg[&ik_c\left(1+\gamma^2+2\frac{U_c-c_g}{U_c-c}+2\gamma^2\frac{U_c+c_g}{U_c+c}\right) + r\left(\frac{1}{U_c-c}-\frac{\gamma^2}{U_c+c}\right)\\ &+\frac{\left(U_c-c_g\right)Z+Y}{ik_cF}\left(F\frac{U_c-c_g}{U_c-c} - \left(K_c^2+F\right)\gamma\frac{U_c+c_g}{U_c+c}+\gamma Y'\right)\Bigg]\end{aligned} \tag{40}$$

$$\begin{aligned}\zeta = \frac{ik_cK_c^2}{8\left(Z+\gamma^2Z'\right)}\Bigg[&\frac{4\pi^2+3F}{\left(U_c-c\right)^2} + \frac{\gamma^2\left|\gamma\right|^2\left(4\pi^2+3F\right)}{\left(U_c+c\right)^2} + \frac{3F\left(\left|\gamma\right|^2+\gamma^2\right)}{U_c^2-c^2}\\ &+\frac{3\gamma^2\left|\gamma\right|^2Z'}{U_c+c} - \frac{3Z}{U_c-c}\Bigg].\end{aligned} \tag{41}$$

where

$$\begin{aligned}
Z &= \frac{\beta+2FU_c}{(U_c-c)^2}+i\frac{r}{k_c}\frac{K_c^2}{(U_c-c)^2},\\
Z' &= \frac{\beta-2FU_c}{(U_c+c)^2}+i\frac{r}{k_c}\frac{K_c^2}{(U_c+c)^2},\\
Y &= 2k_c^2-\frac{\beta+2FU_c+2ik_cr}{U_c-c},\\
Y' &= 2k_c^2+\frac{\beta-2FU_c+2ik_cr}{U_c+c}.
\end{aligned}$$

4 Parameter Regime Analysis

Having computed the coefficients of equation (35) in terms of physical variables, we are now prepared to determine which of the qualitative dynamics of the CGL observed numerically in [1] and [12] may be observable in baroclinic instability.

In [1], Chaté analyzes the CGL in the form

$$\frac{\partial B}{\partial t}=B+(1+ib_1)\frac{\partial^2 B}{\partial x^2}-(b_3-i)\left|B\right|^2 B. \tag{42}$$

where b_1, b_3 are real and $b_3>0$. This simple form is obtained from equation (35) by making the transformations

$$t=\mathbb{R}\mathrm{e}\{\mu\}\tau,\quad x=\sqrt{\tfrac{\mathbb{R}\mathrm{e}\{\mu\}}{\mathbb{R}\mathrm{e}\{\nu\}}}\eta,\quad B(x,t)=\sqrt{-\tfrac{\mathbb{I}\mathrm{m}\{\zeta\}}{\mathbb{I}\mathrm{m}\{\mu\}}}e^{-i\frac{\mathbb{I}\mathrm{m}\{\mu\}}{\mathbb{R}\mathrm{e}\{\mu\}}t}A\left(\sqrt{\tfrac{\mathbb{R}\mathrm{e}\{\nu\}}{\mathbb{R}\mathrm{e}\{\mu\}}}x,t/\mathbb{R}\mathrm{e}\{\mu\}\right),$$

from which we find

$$b_1 = -\operatorname{sgn}(\mathbb{I}\mathrm{m}\{\zeta\})\frac{\mathbb{I}\mathrm{m}\{\nu\}}{\mathbb{R}\mathrm{e}\{\nu\}}, \tag{43}$$

$$b_3 = \left|\frac{\mathbb{R}\mathrm{e}\{\zeta\}}{\mathbb{I}\mathrm{m}\{\zeta\}}\right|. \tag{44}$$

Thus, the parameter space of the CGL has two real dimensions.[1]

The qualitatively different regimes of parameter space are mapped with respect to b_1 and b_3 in figure 3a. This figure is reproduced from [1]. To discover which regimes are relevant to baroclinic instability, b_1 and b_3 were computed numerically for a range of β, r, and F.

It was found that b_1, b_3 are functions of F and β/r only, though this fact is not immediately obvious from the formulas for ζ and ν. For all tested values of F, β/r, we found $b_1\le 0$. At fixed F, decreasing β/r increases b_3 and decreases $|b_1|$. As β/r is varied, the coefficients roughly satisfy $b_1b_3=C(F)$. Decreasing F at fixed β/r also increases b_3 and decreases $|b_1|$. In the limit that $\beta/r\to 0$ or $F\to\pi^2/2$, we find that $b_3\to\infty$ and $b_1\to 0$. [2] In this limit,

[1]Technically, this form can be obtained from equation (35) only if $\mathbb{I}\mathrm{m}\{\zeta\}<0$, as is apparent from an inspection of the transformations. However, if $\mathbb{I}\mathrm{m}\{\zeta\}>0$, taking the complex conjugate of equation (1) and then applying the transformations yields equation (42) for $\overline{B}$.

[2]Recall from §3 that for $F\le\pi^2/2$, baroclinic instability is impossible.

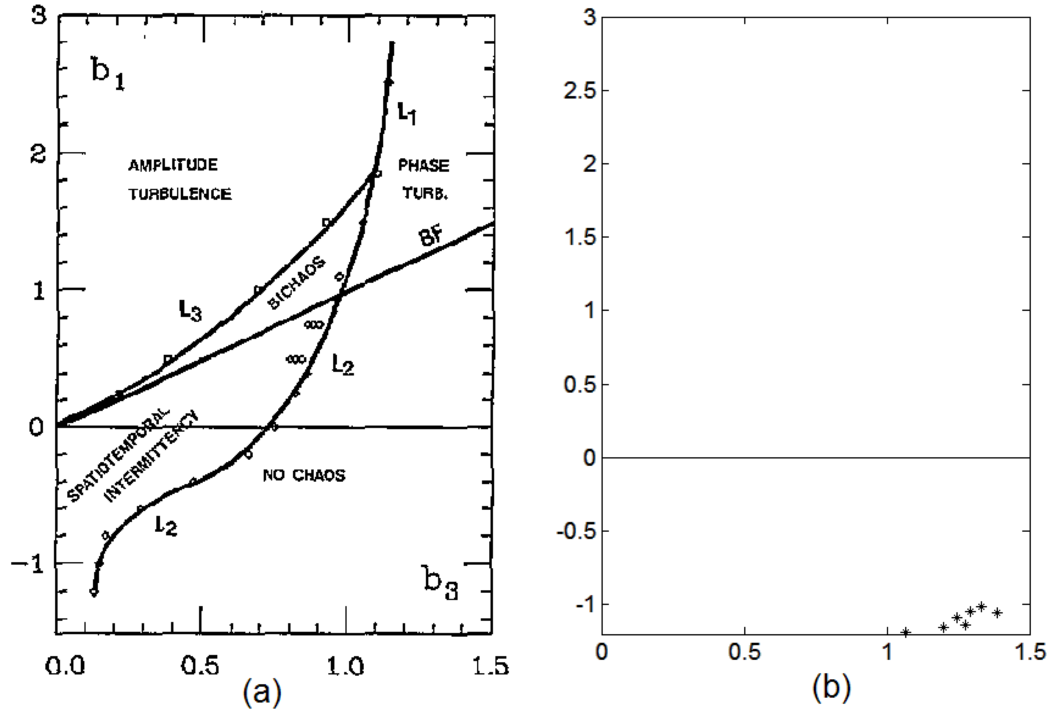

Figure 3: (a) The parameter regime diagram of the CGL produced by Chaté, Shraiman, et al. Reproduced from [1]. (b) These points represent the only points for $5 < F < 50$ and $0.1 < \beta/r < 50$ that fall in the sector of parameter space studied in [1], [12]. The points correspond to $\beta/r \approx 10 - 40$ and fall well within the "no chaos" regime.

the coefficients of the CGL are purely real. The real Ginzburg-Landau equation, unlike its complex cousin, is derivable from a variational principle, and its solutions always relax to a stationary equilibrium state.

The values of b_1 and b_3 for $5 < F < 50$ and $0.1 < \beta/r < 50$ are plotted in figure 4. The lower limits of these ranges were chosen to exclude divergent values of b_3 as $F \to \pi^2/2 \approx 4.93$ and $\beta/r \to 0$. An upper limit of 50 was chosen for both F and β/r to prevent these parameters from being much more than an order of magnitude larger than one. It is implicit in the derivation of equation (35) that $F, \beta, r \ll |\Delta|^{-1/2}$. The larger these parameters become, the smaller $|\Delta|$ must be for equation (35) to be asymptotically consistent.

As baroclinic instability resides exclusively in the region $b_1 \leq 0$, we focus on the dynamical regimes present there. For $b_1 < b_3$, a band of stable plane wave solutions[3] of the form

$$B = \tilde{B}(k)e^{i(kx-\omega(k)t)}$$

exists with $\tilde{B}^2 = \left(1 - k^2\right)/b_3$ and $\omega = 1/b_3 - (b_1 + 1/b_3)k^2$. These solutions are linearly

[3]When $b_1 = b_3$, this band of wavenumbers vanishes, and stable monochromatic plane wave solutions cease to exist. This bifurcation is known as the Benjamin-Feir instability of the $k = 0$ state. The turbulent regimes in the Benjamin-Feir unstable region $b_1 > b_3$ are the subject of [12], but because these regimes appear to be inaccessible to baroclinic instability in the Phillips model, we omit discussion of them here.

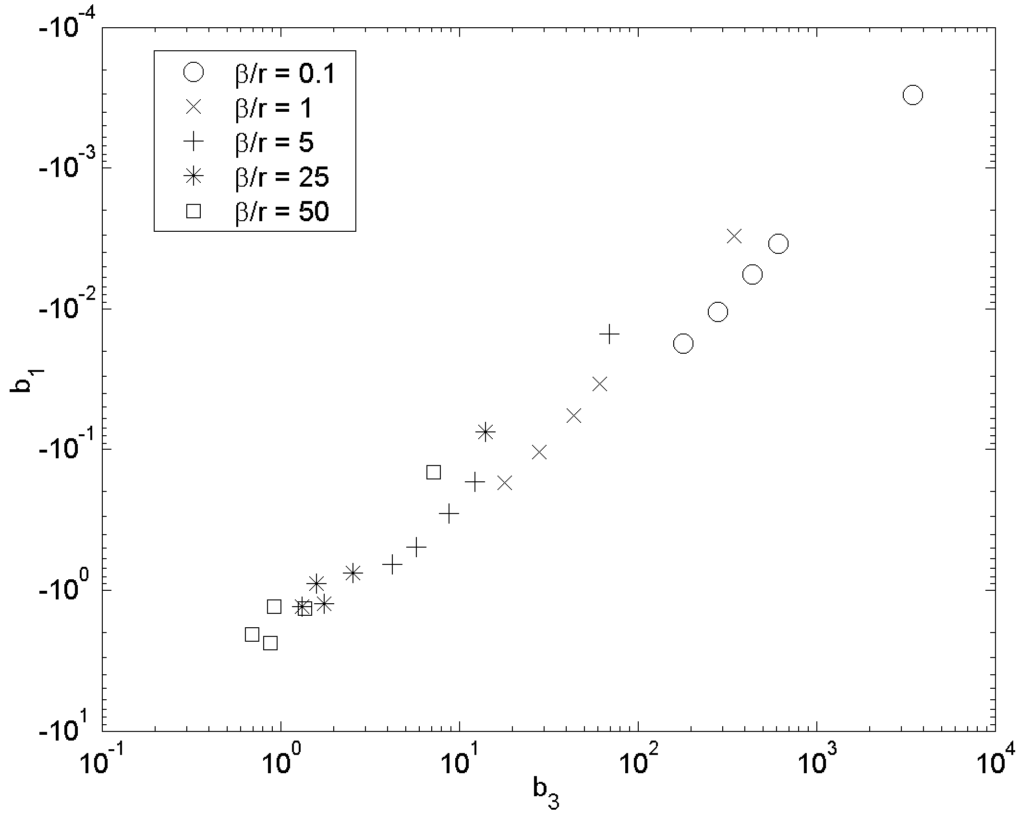

Figure 4: Values of b_1 and b_3 computed for a range of values of β/r and F. Each streak of like-shaped markers corresponds to a fixed value of β/r with $F = 5, 7, 9, 16, 50$. Increasing F with fixed β/r decreases b_3 and increases $|b_1|$. Increasing β/r with fixed F yields the same trend, but the dependence of β/r is stronger than on F.

stable for

$$k^2 < \frac{(b_3 - b_1)}{3b_3 + \frac{2}{b_3} - b_1}.$$

However, the existence of stable plane wave solutions does not preclude the existence of chaotic solutions or localized structures in the same parameter regime. Chaté found that for sufficiently small b_3 solutions could be found numerically in which localized, propagating structures separate large regions of stable plane waves. The structures are characterized by a sharp reduction in $|A|$, and discontinuities or rapid variations in the phase of A. The structures act as nucleation sites for disorder; the stable plane wave regions do not break down until they are contaminated by one of these structures. The nature of these structures is discussed in the context of known exact solutions of the CGL at some length in [1] and [13].

However, it is not yet clear whether these structures can be expected to appear in baroclinic instability. For the range of β, r, and F, tested here, the coefficients b_1, and b_3

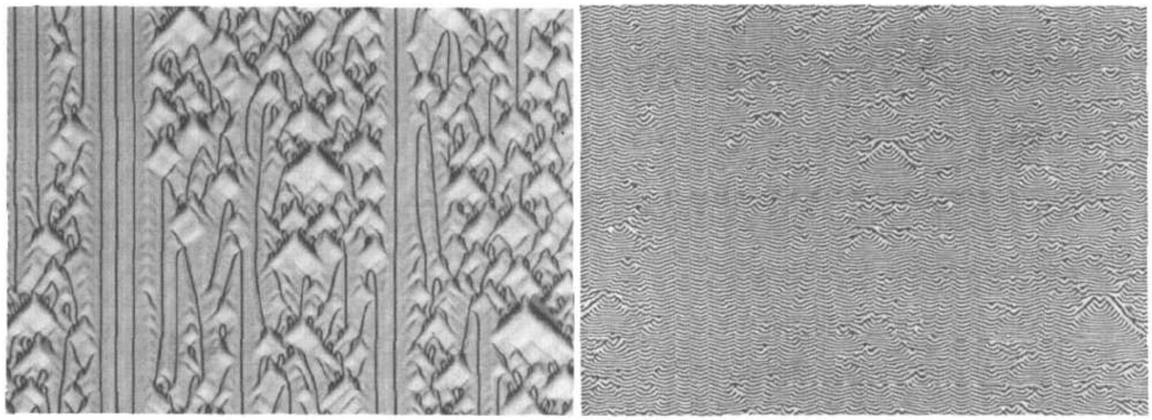

Figure 5: (a) Space-time plot of $|A|$. x increases left to right and t increases upwards. White represents the amplitude maximum $|A| = 2.37$, and black represents $|A| = 0$.
(b) Space-time plot of the phase ϕ of A. Reproduced from [1]. In this run, $b_1 = -0.75$, $b_3 = 0.18$.

generally lie far outside the region of parameter space explored directly by Chaté. Figure 3b shows those parameter values that did lie in that region, and all of those are well within the "no chaos" zone in which intermittency was not observed. For small β/r and F, we have seen that the coefficients asymptote to $b_1 = 0$ and $b_3 = 0$, where the dynamics collapse to those of the real Ginzburg-Landau equation. It is unlikely that disordered states will be discovered in this limit, since solutions of the real Ginzburg-Landau always relax to equilibrium. But as β/r increases, b_3 becomes small. This raises the possibility of intermittency for sufficiently large β/r. However, $|b_1|$ simultaneously becomes large as β/r increases, pushing the coefficients out of the sector of parameter space observed by Chaté. Chaté found that as $|b_1|$ increases, b_3 must be ever smaller for intermittency to be observed. The question, then, is whether b_3 decreases quickly enough to counteract the stabilizing effect of increased $|b_1|$. Furthermore, β/r cannot be increased without bound. We must have $|\Delta|^{1/2} \ll r \ll absdel{-1/2}$ and $\beta \ll |\Delta|^{-1/2}$ for equation (35) to be accurate, and thus $\beta/r \ll |\Delta|$. Numerical simulations of CGL at parameter values appropriate to baroclinic instability are necessary to determine if "baroclinic structures" will emerge or not.

5 Conclusions

We have computed a complex Ginzbug-Landau equation for baroclinic instability in the Phillips model. We have compared the coefficient of this equation to a parameter regime study by Chaté [1] and Shraiman et al [12]. The comparison suggests that, for most physical situations, baroclinic instability should saturate to a monochromatic wave train without intermittency or spatial disorder.

However, the search for baroclinic structures should not be called off yet. The possibility remains that localized structures and spatiotemporal disorder could emerge for large β/r.

Further numerical simulation of the CGL is necessary to determine whether this will happen, as this region of parameter space was not explored in Chaté's paper. In future work, we intend to search for baroclinic structures in numerical solutions of both the CGL and more realistic models of baroclinic instability, such as the Phillips model or a continuously stratified QG model.

6 Acknowledgements

I heartily thank Ed Spiegel, who both introduced me to Pattern theory and pushed me to follow it toward whatever interested me. I also thank Joe Pedlosky for several valuable discussions. I had a wondeful time in Woods Hole this summer, and I want to thank Oliver Bühler and Charles Doering for directing the program.

References

[1] H. Chaté, *Spatiotemporal intermittency regimes of the one-dimensional complex Ginzburg-Landau equation* , Nonlinearity, 7 (1994), pp. 185–204.

[2] P. H. Coullet and E. A. Spiegel, *Amplitude Equations for Systems with Competing Instabilities.*, SIAM Journal on Applied Mathematics, 43 (1983), pp. 776–821.

[3] M. C. Cross and P. C. Hohenberg, *Pattern formation outside of equilibrium*, Reviews of Modern Physics, 65 (1993), pp. 851–1112.

[4] A. E. Gill, *Atmosphere-Ocean Dynamics*, Academic Press, San Diego, California, 1982.

[5] A. C. Newell, T. Passot, and J. Lega, *Order parameter equations for patterns*, Annual Review of Fluid Mechanics, 25 (1993), pp. 399–453.

[6] J. Pedlosky, *Finite-Amplitude Baroclinic Waves.*, J. Atmos. Sci., 27 (1970), pp. 15–30.

[7] ——, *Finite-Amplitude Baroclinic Waves with Small Dissipation.*, J. Atmos. Sci., 28 (1971), pp. 587–597.

[8] ——, *Limit Cycles and Unstable Baroclinic Waves.*, J. Atmos. Sci., 29 (1972), pp. 53–63.

[9] J. Pedlosky, *Geophysical Fluid Dynamics*, Springer Verlag, New York, second ed., 1987.

[10] N. A. Phillips, *Energy transformations and meridional circulations associated with simple baroclinic waves.*, Tellus, 6 (1954), pp. 273–286.

[11] R. D. Romea, *The Effects of Friction and β on Finite-Amplitude Baroclinic Waves.*, J. Atmos. Sci., 34 (1977), pp. 1689–1695.

[12] Shraiman, B. I., Pumir, A. van Saarloos, W. Hohenberg, P. C. Chaté, and M. H. Holen, *Spatiotemporal chaos in the one-dimensional complex Ginzburg-Landau equation*, Physica D Nonlinear Phenomena, 57 (1992), pp. 241–248.

[13] A. Torcini, H. Frauenkron, and P. Grassberger, *Studies of phase turbulence in the one dimensional complex ginzburg-landau equation*, pre, 55 (1997), p. 5073.

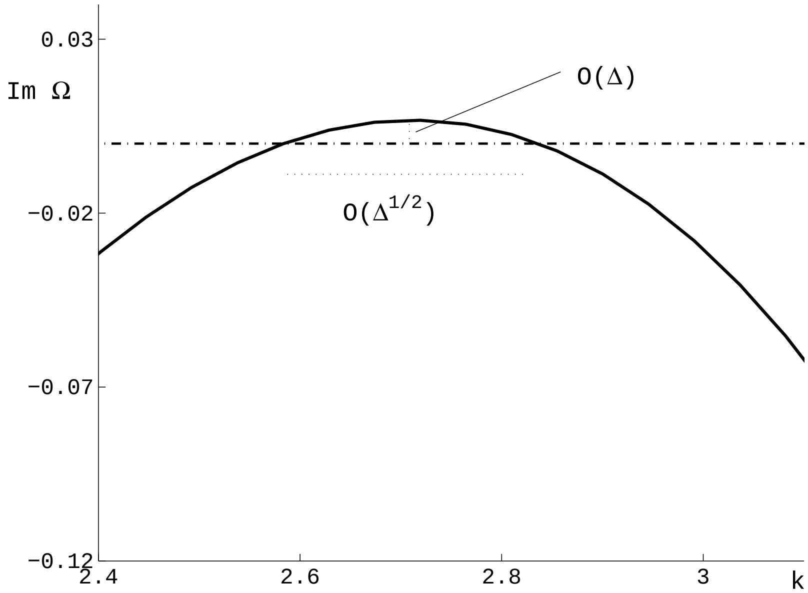

(a)

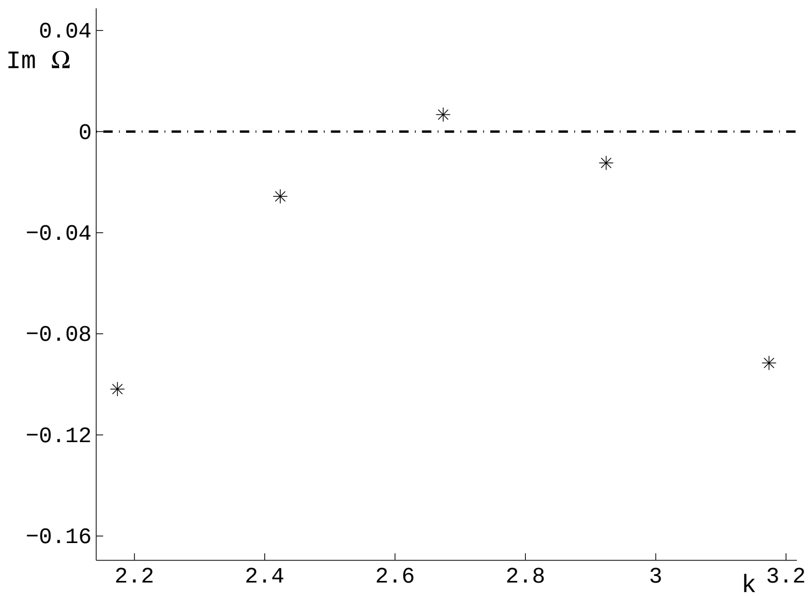

(b)

Figure 6: In both these figures, waves modes' growth rates $\mathbb{Im}\,\{\Omega\}$ are plotted against zonal wavenumber k. (a) When $U = U_c + \Delta$, zooming in around $k = k_c$ reveals a band of unstable wavenumbers k with growth rates of $O(\Delta)$. The unstable band has width $O\left(|\Delta|^{1/2}\right)$.
(b) When the channel has finite length, only a discrete spectrum of wavenumbers k are allowed. In this case, one mode may become unstable alone, while all others remain stable.